



Technical note UFSM/GruMA 001/2023

Turbulent Kinetic Energy Budget for MYNN-EDMF PBL Scheme in WRF model

Franciano Scremin Puhales^{1a,1b,*}, Joseph B. Olson², Jimmy Dudhia³, Douglas Lima de Bem^{1a}, Rafael Maroneze^{1b,4}, Otávio Costa Acevedo^{1b}, Felipe Denardin Costa^{1b,4}, and Vagner Anabor^{1a}

^{1a}Universidade Federal de Santa Maria (UFSM) – Grupo de Turbulência Atmosférica, Santa Maria, Rio Grande do Sul, Brazil

^{1b}Universidade Federal de Santa Maria (UFSM) – Grupo de Modelagem Atmosférica, Santa Maria, Rio Grande do Sul, Brazil

²National Oceanic and Atmospheric Administration (NOAA) – Earth System Research Laboratory, Boulder, Colorado, US

³National Center for Atmospheric Research (NCAR) – Mesoscale & Microscale Meteorology Laboratory, Boulder, Colorado, US

⁴Universidade Federal do Pampa (Unipampa) – Laboratório de Fluidodinâmica Computacional e turbulência Atmosférica, Alegrete, Rio Grande do Sul, Brazil

*Corresponding author: franciano.puhales@ufsm.br

Santa Maria, Rio Grande do Sul, Brazil

2023

CONTENTS

1	MYNN-EDMF's TKE Budget Equation	2
1.1	Production terms	3
1.2	Vertical transport term	5
1.3	TKE dissipation rate	5
2	New stability functions for MYNN	6
A	WRF staggered grid	8

TECHNICAL NOTE'S AIM

1 The aim of this technical note is to describe the Turbulent Kinetic Energy (TKE) budget equation in Mellor-
 2 Yamada-Nakanishi-Niino (MYNN) PBL scheme of WRF model and how they are outputted. The MYNN scheme
 3 is an improved version of classic Mellor-Yamada scheme (Mellor and Yamada 1982) and it is able to output the
 4 TKE budget equation terms on the default WRF history file. These outputs were unbalanced with the equivalent
 5 terms used on MYNN to integrate the TKE budget equation. It was fixed on WRF 4.2.2 version code for tests
 6 released on WRF 4.5 (CCPP version).

7 Besides the TKE output fix, a new set of similarity relationship equations was implemented in the MYNN
 8 scheme to provide the lower boundary conditions for TKE budget equation terms.

1 MYNN-EDMF'S TKE BUDGET EQUATION

In MYNN-EDMF, the Q Budget equation is given by (Nakanishi and Niino 2009; Olson et al. 2019):

$$\frac{\partial Q}{\partial t} = T_{rq} + P_{sq} + P_{bq} + D_q \quad (1.1)$$

9 where $Q = q^2 = 2e$ is twice the TKE e , and T_{rq} , P_{sq} , P_{bq} , and D_q are the vertical transport, shear production,
 10 buoyancy production/destruction, and dissipation rates of Q respectively. As $Q = 2e$, therefore:

$$\begin{aligned} \frac{\partial e}{\partial t} &= \frac{1}{2}T_{rq} + \frac{1}{2}P_{sq} + \frac{1}{2}P_{bq} + \frac{1}{2}D_q \\ \frac{\partial e}{\partial t} &= T_r + P_s + P_b + D \end{aligned} \quad (1.2)$$

11 where the right side of equation 1.2 has the analogous terms of 1.1 related to TKE.

Equation 1.1 is solved using an implicit time-integration method and it is discretized as follows:

$$\underbrace{\frac{Q_{k+1/2}^{n+1} - Q_{k+1/2}^n}{\Delta t}}_{\text{TKE tendency}} = \underbrace{\frac{\partial}{\partial z} \left[K_q^n \frac{\partial}{\partial z} (Q^{n+1}) \right]_{k+1/2}}_{\text{Eddy difusivity}} + \underbrace{\frac{\partial}{\partial z} \left[M^n (Q^{n+1} - Q_u^n) \right]_{k+1/2}}_{\text{Mass-flux transport}} + \underbrace{P_{k+1/2}^n}_{\text{TKE turbulent Production Destruction}} - \underbrace{F_{k+1/2}^n Q_{k+1/2}^{n+1}}_{\text{Dissipation rate}} \quad (1.3)$$

TKE transport

where n denotes the time index and k denotes the vertical level index. As the WRF grid is staggered, the full levels (cell faces) are represented by the integer k index, while the half levels are represented by $k + 1/2$ index levels (for further details see appendix A). In equation 1.3, Q is a half level variable, while K_q and M are full level variables. Furthermore, the first and second terms of the right side are the eddy diffusion and mass-flux Q transport terms, P is the sum of shear and buoyancy terms, and the last term FQ is the dissipation rate. The time-integration of equation 1.3 is solved by the following relationship:

$$aQ_{k-1/2}^{n+1} + bQ_{k+1/2}^{n+1} + cQ_{k+3/2}^{n+1} = d \quad (1.4)$$

12 where a , b , and c are the matrix elements to solve the implicit system for $Q_{k-1/2}^{n+1}$.

13 To output all TKE budget equation terms in wrfout_d<domain>_AAAA-MM-DD_HH:mm files, it is necessary
 14 to use the bl_mynn_tkebudget(maxdom) variable in &physics block of namelist.input file:

$$\text{bl_mynn_tkebudget(maxdom)} = \begin{cases} 0, & \text{not outputted (default)} \\ 1, & \text{outputted} \end{cases}$$

15 The output variables associated to TKE budget equation are:

Table 1.1 – Summary of TKE budget equation variables outputted in wrfout_d<domain>_AAAA-MM-DD_HH:mm files.

TKE Budget term	Variable name	Description
Mechanical production	QSHEAR	TKE Production - shear
Buoyancy production/destruction	QBUOY	TKE Production - buoyancy
TKE vertical transport	QWT	TKE vertical transport
TKE dissipation rate	QDISS	TKE dissipation
TKE tendency	DTKE	TKE tendency

16 In this WRF version, all outputted TKE budget variables are obtained as a “mass” grid point variable (see
 17 appendix A for more details).

18 1.1 Production terms

The TKE production¹ terms are given by:

$$P_s = -\langle u'w' \rangle \frac{\partial u}{\partial z} - \langle v'w' \rangle \frac{\partial v}{\partial z} \quad (1.5)$$

$$P_b = \frac{g}{\theta_0} \langle w'\theta'_v \rangle \quad (1.6)$$

19 since $g = 9,81 \text{ m s}^{-2}$ is the gravity acceleration and $\theta_0 = 300 \text{ K}$ is the reference potential temperature.

The turbulent fluxes are evaluated from local-gradient and counter-gradient terms (Nakanishi and Niino 2009; Olson et al. 2019):

$$\langle w'\phi' \rangle = -K_{h,m} \left(\frac{\partial \phi}{\partial z} - \gamma \right) \quad (1.7)$$

For the momentum fluxes, $\gamma = 0$ and $K_m = \ell q S_m$ were considered, while for scalar fluxes $K_h = \ell q S_h$ was employed. Also, $\langle w'\theta'_v \rangle$ is divided in two terms, local (L) and a non-local (NL) (Olson et al. 2019):

$$\langle w'\theta'_v \rangle = \langle w'\theta'_v \rangle^L + \langle w'\theta'_v \rangle^{NL} \quad (1.8)$$

20

¹ P_b is a production or destruction term depending on the static stability.

In equation 1.3, $P_{k+1/2}^n$ is given by:

$$P_{k+1/2}^n = P_{s_{i+1/2}}^n + P_{b_{i+1/2}}^n \quad (1.9)$$

$$P_{s_{k+1/2}}^n = \frac{1}{2} (P_{s_k}^n + P_{s_{k+1}}^n) \quad (1.10)$$

$$P_{b_{k+1/2}}^n = \frac{1}{2} (P_{b_k}^n + P_{b_{k+1}}^n) \quad (1.11)$$

21

22 For $k > 0$:

$$P_{s_k} = \ell_k q_k S_{m_k} g_{m_k} \quad (1.12)$$

$$g_{m_k} = \frac{(u_{k+1/2} - u_{k-1/2})^2 - (v_{k+1/2} - v_{k-1/2})^2}{\Delta z_{k-1/2}^2} \quad (1.13)$$

$$P_{b_k} = -\ell_k q_k (S_{h_k} g_{h_k} - \gamma \theta) + P_{bnl_k} \quad (1.14)$$

$$g_{h_k} = \frac{(\theta_{v_{k+1/2}} - \theta_{v_{k-1/2}})}{\Delta z_{k-1/2}} \frac{g}{\theta_0} \quad (1.15)$$

$$(1.16)$$

23 where P_{bnl_k} is the non-local TKE buoyancy production/destruction. Since q is a half-level variable, q_k is obtained
 24 by a linear interpolation of $q_{k-1/2}$ and $q_{k+1/2}$. Furthermore, the vertical grid spacing between full and half levels
 25 are given by:

$$\Delta z_k = z_{k+1} - z_k \quad (1.17a)$$

$$\Delta z_{k+1/2} = \frac{1}{2} (\Delta z_k + \Delta z_{k+1}) \quad (1.17b)$$

26 where $z_k = 0$ since $k = 0$.

27 Similarity relationships are used as lower boundary condition to obtain these terms for $k = 0$:

$$P_{s_k} = 2 \left(\frac{u_*^3}{\kappa z_{1/2}} \right) \phi_m - P_{s_{k+1}} \quad (1.18)$$

$$P_{b_k} = 2 \left(\frac{u_*^3}{\kappa z_{1/2}} \right) \zeta - P_{b_{k+1}} \quad (1.19)$$

28

29 where u_* is the friction velocity, $\zeta = \frac{z_{1/2}}{L}$ is the stability parameter, L is the Monin-Obukhov length, ϕ_m is a stability
 30 function, $z_{1/2} = \left(\frac{1}{2} \right) \Delta z_1$, and $\kappa = 0.4$ is the von Karman constant.

31 The MYNN has used a Kansas-type similarity gradient function to prescribe the TKE production at the first
 32 vertical half level, given by (Arya 2001):

$$\phi_{mK} = \begin{cases} (1 - a_{mK}\zeta)^{-1/4}, & \text{if } \zeta < 0 \\ (1 + b_{mK}\zeta), & \text{if } \zeta \geq 0 \end{cases} \quad (1.20)$$

where $a_{mk} = 16$, $b_{mk} = 5$, and ζ has its value updated inside MYNN with the surface heat flux obtained from LSM (land-surface model), as follows:

$$\zeta = -z_{1/2} \left(\frac{\kappa \frac{g}{\theta_0} \langle w' \theta'_v \rangle_s}{\max(u_*^3, 1 \times 10^{-6})} \right) \quad (1.21)$$

33
34 A new stability function was implemented in WRF 4.2.2 as a testing option and it is described in section 2. This
35 new option is based on Jiménez et al. (2012) stability functions for profile relationships. This new set of equations
36 working in the same ζ domain that ones used on MM5 revised and MYNN surface layer (SFCLAY) modules,
37 which are compatible with MYNN PBL scheme.

38 1.2 Vertical transport term

The vertical transport term is divided in an eddy diffusivity (ED , local) and a mass-flux (MF , non-local) terms:

$$T_{r_{k+1/2}}^n = ED_{k+1/2}^n + \gamma_{MF} MF_{k+1/2}^n \quad (1.22a)$$

$$ED_{k+1/2}^n = \frac{1}{2\Delta z_k} \left[\frac{K_{q_{k+1}}^n}{\Delta z_{k+1/2}} \left(Q_{k+3/2}^{n+1} - Q_{k+1/2}^{n+1} \right) - \frac{K_{q_i}^n}{\Delta z_{k-1/2}} \left(Q_{k+1/2}^{n+1} - Q_{k-1/2}^{n+1} \right) \right] \quad (1.22b)$$

$$MF_{k+1/2}^n = \frac{1}{\Delta z_k} \left[\left(\frac{M_{k+1}^n}{2} \right) Q_{k+3/2}^{n+1} + \left(\frac{M_{k+1}^n - M_k^n}{2} \right) Q_{k+1/2}^{n+1} - \left(\frac{M_k^n}{2} \right) Q_{k-1/2}^{n+1} + M_k^n Q_{u_k}^n - M_{k+1}^n Q_{u_{k+1}}^n \right] \quad (1.22c)$$

39 where $\gamma_{MF} = 0$ or 1 is a activation parameter that controls the MF term. It is changed in the namelist file trough
40 the variable `bl_mynn_edmf_tke(maxdom)`, as follows:

$$\text{bl_mynn_edmf_tke(maxdom)} = \begin{cases} 0, & \gamma_{MF} = 0: \text{MF term is turned off (default)} \\ 1, & \gamma_{MF} = 1: \text{MF term is activated} \end{cases}$$

41 1.3 TKE dissipation rate

The TKE dissipation rate is given by:

$$\epsilon_{k+1/2}^n = -\frac{1}{2} F_{k+1/2}^n Q_{k+1/2}^{n+1} \quad (1.23)$$

where $F_{k+1/2}^n = \frac{q_{k+1/2}^n}{b_1 \ell_{k+1/2}^n}$, $b_1 = 24$ (Nakanishi and Niino 2009). The mixing length is a full-level variable. At half levels, it is given by:

$$\ell_{k+1/2}^n = \frac{1}{2} (\ell_k^n + \ell_{k+1}^n) \quad (1.24)$$

42
43 Furthermore, for $k = 0$: $\ell_k^n = 0$.

2 NEW STABILITY FUNCTIONS FOR MYNN

44 The new gradient relationship is given by

$$\phi_\alpha = \begin{cases} \phi_{\alpha g} = 1 - \zeta \frac{d\psi_{\alpha g}}{d\zeta}, & \text{if } \zeta < 0 \\ \phi_{\alpha c} = 1 + a_{\alpha c} \frac{\zeta + \zeta^{b_{\alpha c}} (1 + \zeta^{b_{\alpha c}})^{b_{\alpha c}^{-1} - 1}}{\zeta + (1 + \zeta^{b_{\alpha c}})^{b_{\alpha c}^{-1}}}, & \text{if } \zeta \geq 0 \end{cases} \quad (2.1)$$

45 where $\alpha = m, h$ identify the function for momentum (m) and heat (h), $\phi_{\alpha g}$ is the gradient similarity obtained from
46 Grachev et al. (2000) expression for $\psi_{\alpha g}$. The constants $a_{\alpha c}$ and $b_{\alpha c}$ are presented in table 2.1 (Cheng and Brutsaert
47 2005):

Table 2.1 – Constants used in the new gradient relationship for neutral/stable regimes.

α	$a_{\alpha c}$	$b_{\alpha c}$
m	6.1	2.5
h	5.3	1.1

For both stability conditions, the similarity relationship profiles used by Jiménez et al. (2012) are related to gradient functions as follows:

$$\psi_\alpha(\zeta) = \int_0^\zeta \frac{1 - \phi_\alpha(\zeta)}{\zeta} d\zeta \quad (2.2)$$

48 The relationship between gradient and profile stability functions is used to obtain the first one for unstable regime ($\zeta < 0$). In this case, the profile relationship is given by (Grachev et al. 2000; Jiménez et al. 2012):

$$\psi_{\alpha g}(\zeta) = \frac{\psi_{\alpha K} + \zeta^2 \psi'_{\alpha g}}{1 + \zeta^2} \quad (2.3)$$

49 where $\psi_{\alpha K}$ is the Kansas-type profile relationship (Arya 2001),

$$\psi_{\alpha K} = \begin{cases} 2\ln\left(\frac{1+x}{2}\right) + \ln\left(\frac{1+x^2}{2}\right) - 2\arctan(x) + \frac{\pi}{2}, & \alpha = m \\ 2\ln\left(\frac{1+x^2}{2}\right), & \alpha = h \end{cases} \quad (2.4)$$

where $x = (1 - a_{\alpha K})^{1/4}$, $a_{\alpha K} = a_{mK} = a_{hK} = 16$, and $\psi'_{\alpha g}$ is given by the following expression:

$$\psi'_{\alpha g}(\zeta) = \frac{3}{2} \ln\left(\frac{y_{\alpha}^2 + y_{\alpha} + 1}{3}\right) - \sqrt{3} \arctan\left[\frac{\sqrt{3}}{3}(2y_{\alpha} + 1)\right] + \frac{\sqrt{3}\pi}{3} \quad (2.5)$$

50 where $y_{\alpha} = (1 - r_{\alpha}\zeta)^{1/3}$, with $r_m = 10$ and $r_h = 34$.

51 From equation 2.3:

$$\begin{aligned} \frac{d\psi_{\alpha g}}{d\zeta} &= \frac{\left[\frac{d}{d\zeta}(\psi_{\alpha K}) + \zeta^2 \psi'_{\alpha g}(1 + \zeta^2) - (\psi_{\alpha K} + \zeta^2 \psi'_{\alpha g}) \frac{d}{d\zeta}(1 + \zeta^2) \right]}{(1 + \zeta^2)^2} \\ \frac{d\psi_{\alpha g}}{d\zeta} &= \frac{\frac{1 - \phi_{\alpha K}}{\zeta} + 2\zeta \psi'_{\alpha g} + \zeta^2 \frac{d\psi'_{\alpha g}}{d\zeta}}{(1 + \zeta^2)} \end{aligned} \quad (2.6)$$

52 where $\phi_{\alpha K}$ the Kansas-type gradient similarity relationship (equation 1.20).

Substituting the functions $f_{\alpha} = \frac{1}{3}(y_{\alpha}^2 + y_{\alpha} + 1)$ and $g_{\alpha} = \frac{\sqrt{3}}{3}(2y_{\alpha} + 1)$ in $\psi'_{\alpha g}$ it is possible to obtain the following relationships:

$$\psi'_{\alpha g} = \frac{3}{2} \ln(f_{\alpha}) - \sqrt{3} \arctan(g_{\alpha}) + \frac{\sqrt{3}\pi}{3} \quad (2.7a)$$

$$\frac{d\psi'_{\alpha g}}{d\zeta} = \frac{3}{2} \frac{1}{f_{\alpha}} \frac{df_{\alpha}}{d\zeta} - \sqrt{3} \left(\frac{1}{1 + g_{\alpha}^2} \right) \frac{dg_{\alpha}}{d\zeta} \quad (2.7b)$$

$$\frac{df_{\alpha}}{d\zeta} = \frac{1}{3} \frac{dy_{\alpha}}{d\zeta} (2y_{\alpha} + 1) \quad (2.7c)$$

$$\frac{dg_{\alpha}}{d\zeta} = \frac{2\sqrt{3}}{3} \frac{dy_{\alpha}}{d\zeta} \quad (2.7d)$$

$$\frac{dy_{\alpha}}{d\zeta} = -\frac{r_{\alpha}}{3} (1 - r_{\alpha}\zeta)^{-2/3} \quad (2.7e)$$

53 In this way, the gradient similarity relationship for $\zeta < 0$ is obtained by substituting equations 2.5, 2.6, and 2.7 in
54 equation 2.1.

55 Figure 2.1 exhibits a comparison between the Kansas-type and the new gradient similarity relationships. An
56 advantage of the new functions is the ζ domain for which $\phi_{\alpha}(\zeta)$ is properly defined. In general, The Kansas-type
57 functions were obtained from experimental data interpolated in $-2 \geq \zeta \geq 1$. Thus, the new functions can be used
58 in larger stability domain values.

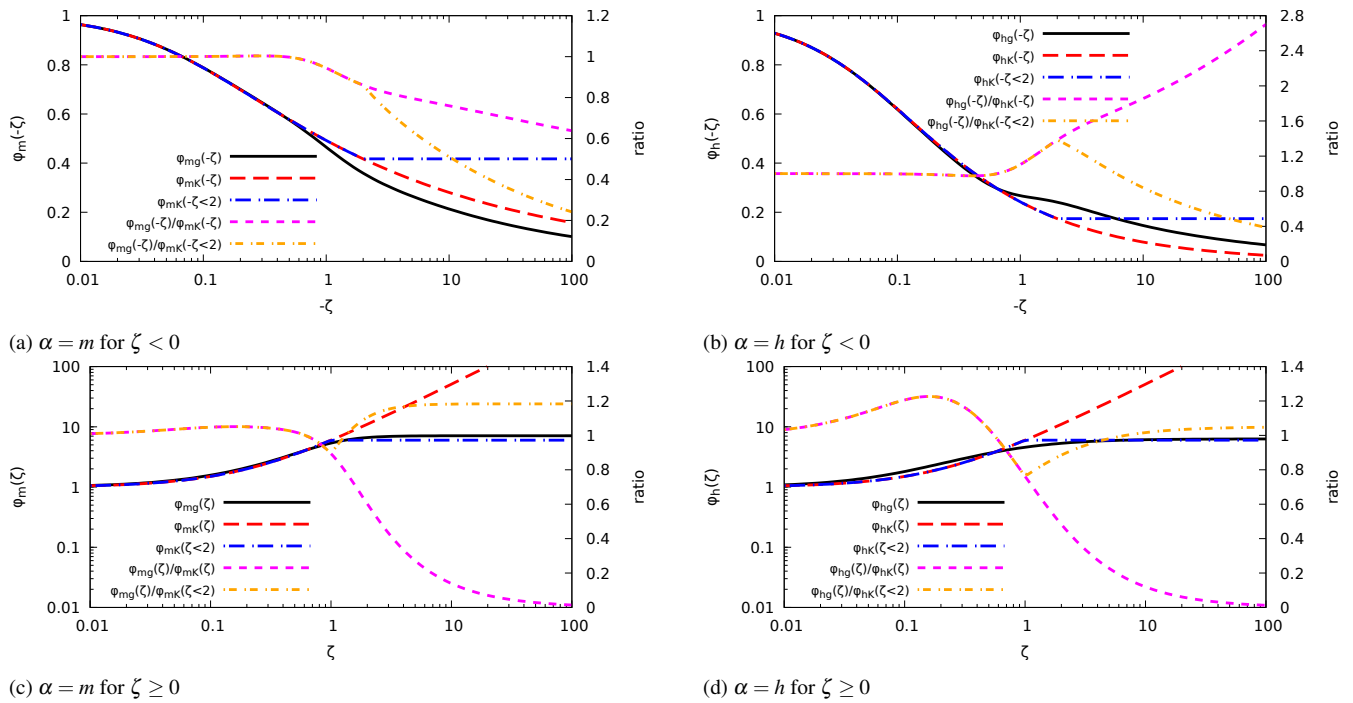


Figure 2.1

59 The stability function option `bl_mynn_stfunc` is hard-coded in WRF. It must be changed near the top of the
60 `module_bl_mynn.F` before compiling, as follows:

$$\text{bl_mynn_stfunc} = \begin{cases} 0, & \text{Kansas-type (default)} \\ 1, & \text{new option (for testing)} \end{cases}$$

61 The default option is `bl_mynn_stfunc = 1`.

A WRF STAGGERED GRID

62 The WRF grid is an Arakawa C grid where the center-cell grid points are called “mass points”. The face grid
63 points staggered at one-half grid length from the mass points are called U, V, and W points. These faces are normal
64 to these wind speed components (Skamarock et al. 2019). Figure A.1 shows a 3D view of a WRF grid cell where
65 the mass and wind points are identified. The center and face points are staggered for $\frac{1}{2}\Delta x_i$, where Δx_i is the mesh
66 resolution in i direction, the index $\alpha + 1/2$ and $\alpha - 1/2$ denotes points that are at $\pm \frac{1}{2}\Delta x_i$ from α .

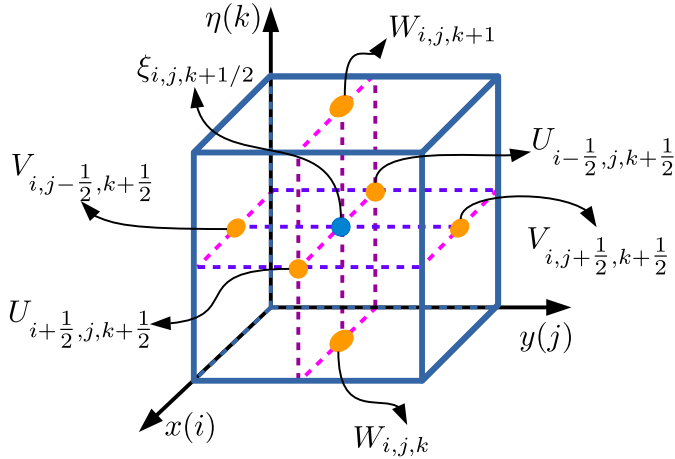


Figure A.1 – Representation of a WRF grid cell. The face-yellow dots are related to wind points while the centered-blue dot is the mass grid point.

67 In a vertical column of WRF grid, the TKE budget equation terms obtained on grid cell vertical faces (W points)
 68 are converted to centred point values by an average procedure. For any variable A_k and $A_{k\pm 1}$, the center grid point
 69 value $A_{k\pm 1/2}$ is given as follows:

$$A_{k\pm\frac{1}{2}} = \frac{A_k + A_{k\pm 1}}{2} \quad (\text{A.1})$$

BIBLIOGRAPHY

- 70 Arya, S. P., 2001: *Introduction to micrometeorology*. 2nd ed., Academic Press, San Diego, 420 pp.
- 71 Cheng, Y., and W. Brutsaert, 2005: Flux-profile relationships for wind speed and temperature in the stable atmo-
 72 spheric boundary layer. *Bound.-Lay. Meteorol.*, **114**, 519–538, doi:10.1007/s10546-004-1425-4.
- 73 Grachev, A., C. Fairall, and E. Bradley, 2000: Convective profile constants revisited. *Bound.-Lay. Meteorol.*, **94** (3),
 74 495–515, doi:10.1023/A:1002452529672.
- 75 Jiménez, P. A., J. Dudhia, J. F. González-Rouco, J. Navarro, J. P. Montávez, and E. García-Bustamante, 2012:
 76 A revised scheme for the wrf surface layer formulation. *Mon. Weather Rev.*, **140** (3), 898–918, doi:10.1175/
 77 MWR-D-11-00056.1.
- 78 Mellor, G. L., and T. Yamada, 1982: Development of a turbulence closure model for geophysical fluid problems.
 79 *Reviews of Geophysics and Space Physics*, **20** (4), 851–875.
- 80 Nakanishi, M., and H. Niino, 2009: Development of an improved turbulence closure model for the atmospheric
 81 boundary layer. *J. Meteorol. Soc. Jpn.*, **87** (5), 895–912, doi:10.2151/jmsj.87.895.
- 82 NCAR-MMM, 2020: Weather forecast and research model. National Center for Atmospheric Research, URL
 83 https://www2.mmm.ucar.edu/wrf/users/docs/user_guide_v4/contents.html, accessed Nov 15, 2020.
- 84 Olson, J. B., J. S. Kenyon, W. M. Angevine, J. M. . Brown, M. Pagowski, and K. Sušelj, 2019: *A Description*
 85 *of the MYNN-EDMF Scheme and the Coupling to Other Components in WRF-ARW*. Boulder, URL 10.25923/
 86 n9wm-be49.
- 87 Skamarock, W. C., and Coauthors, 2019: *A Description of the Advanced Research WRF Version 4*. Boulder, doi:
 88 10.5065/1dfh-6p97.